# The $D_3$ fold mechanism in the Joma mine district, Leipikvattnet Nappe, Nord-Trøndelag, Norway

BRIAN MARSHALL

In the area of the Joma mine (Nord-Trøndelag, Norway), $D_3$ folds have been ascribed to either across-layer inhomogeneous simple shear or flexural processes modified by pure shear. The former was based on a near great-circle redistribution of $D_2$ linear elements by $D_3$; the latter was mainly based on the $D_3$ fold style. Considerations of basic theory and of fold and redistribution geometries at Joma show that: near great-circle redistributions of previously rectilinear elements do not prove simple shear folding; fold styles and dip isogon patterns are incompatible with true similar geometry and a dominantly simple shear fold mechanism; and the pre-$D_3$ geometry of form-surface and contained linear elements precludes a simple great-circle redistribution pattern. The $D_3$ geometry reflects buckling and progressive inhomogeneous contraction as the dominant fold mechanisms. Grossly less competent portions of the regional sequence were dominated by inhomogeneous contraction and allowed near great-circle redistributions. More competent portions were dominated by flexural processes.

*Brian Marshall, Department of Applied Geology, University of Technology, Sydney, P.O. Box 123 Broadway, Australia 2007.*

The Joma Cu–Zn orebody lies within the Leipikvattnet Nappe, part of the Köli Nappe system within the central Scandinavian Caledonides (Kollung 1979; Reinsbakken & Stephens 1986), some 250 km NE of Trondheim (Fig. 1). Marshall et al. (1987), Odling (1988) and Marshall (1990) discussed the structural evolution of the Joma orebody and its immediate hostrocks; Odling (1989) presented the structural history of a larger portion of the nappe centred on the Joma deposit. Although these works are substantially in agreement regarding the sequence of deformation events, Odling (1989) and Marshall (1990) differed in relation to the fold mechanism advocated for the $D_3$ event.

Odling (1989) examined the redistribution of $D_2$ linear fabric elements about the $D_3$ hinge line in terms of what she presented as two end-member folding mechanisms; concentric folding (in fact a geometric rather than mechanistic term) and simple shear folding (a mechanism which yields perfectly similar fold geometry). She stated (1989, fig. 11) that the redistribution pattern most closely approximated the great-circle geometry typical of simple shear folding, rather than the small-circle geometry associated with the concentric model (Fig. 2). Odling (1989) therefore concluded that folding in $D_3$ developed by a dominantly simple shear mechanism.

Marshall (1990) analysed the mesoscale structure of Joma mine. He drew attention to the pre-$D_3$ non-linear distribution of the $D_2$ linear fabric elements, and to the non-plane form surfaces in which $D_3$ folds developed. This was to explain irregular aspects of the geometry of $D_2$ linear elements as redistributed by $D_3$. Marshall (1990) noted, however, that $D_2$ linear elements from surface exposures (derived from Odling 1984, fig. 3) could best be satisfied by a large small-circle redistribution pattern centred on $F_3$ and modified by inhomogeneous pure shear. He suggested that this interpretation was consistent with the $D_3$ fold style (e.g. Marshall & Gilligan 1989 fig. 3; Marshall 1990 , fig. 9C, D) which in no way approached the class 2 geometry (Ramsay 1967) indicative of shear, slip or passive folding (e.g. Donath & Parker 1964; Ramsay 1967).

The present contribution will follow up this difference in interpretation by considering the relationship between perfect similar fold geometry and the across-layer simple shear fold mechanism, and presenting the observed $D_3$ fold geometry in the Joma district.

## Fold mechanism and geometry

The geometry of perfect similar folds can only be explained by across-layer progressive inhomogeneous simple shear, with or without a uniform homogeneous strain (Ramsay 1967, p. 422). The kinematic properties of this mechanism require that an earlier lineation be redistributed within a great-circle which, in the general case, is oblique to the new hinge line and is defined by the original orientation of the lineation and the slip direction (e.g. Ramsay 1960; Turner & Weiss 1963, pp. 482–485).

These relationships have resulted in field-derived great-circle redistribution patterns being equated with shear folding and similar fold geometry (e.g. Turner & Weiss 1963 p. 486; Donath & Parker 1964). But this is a misconception. First, within the limits of field data contoured on an equal-area stereographic net, a redistribution pattern approximating a great-circle can result from fold mechanisms other than across-layer inhomogeneous simple shear (Turner & Weiss 1963, p. 487; Ramsay 1967, pp. 430–436). Second, few natural folds have perfect class 2 similar geometry, and even those which do approximate this form may be explained with-
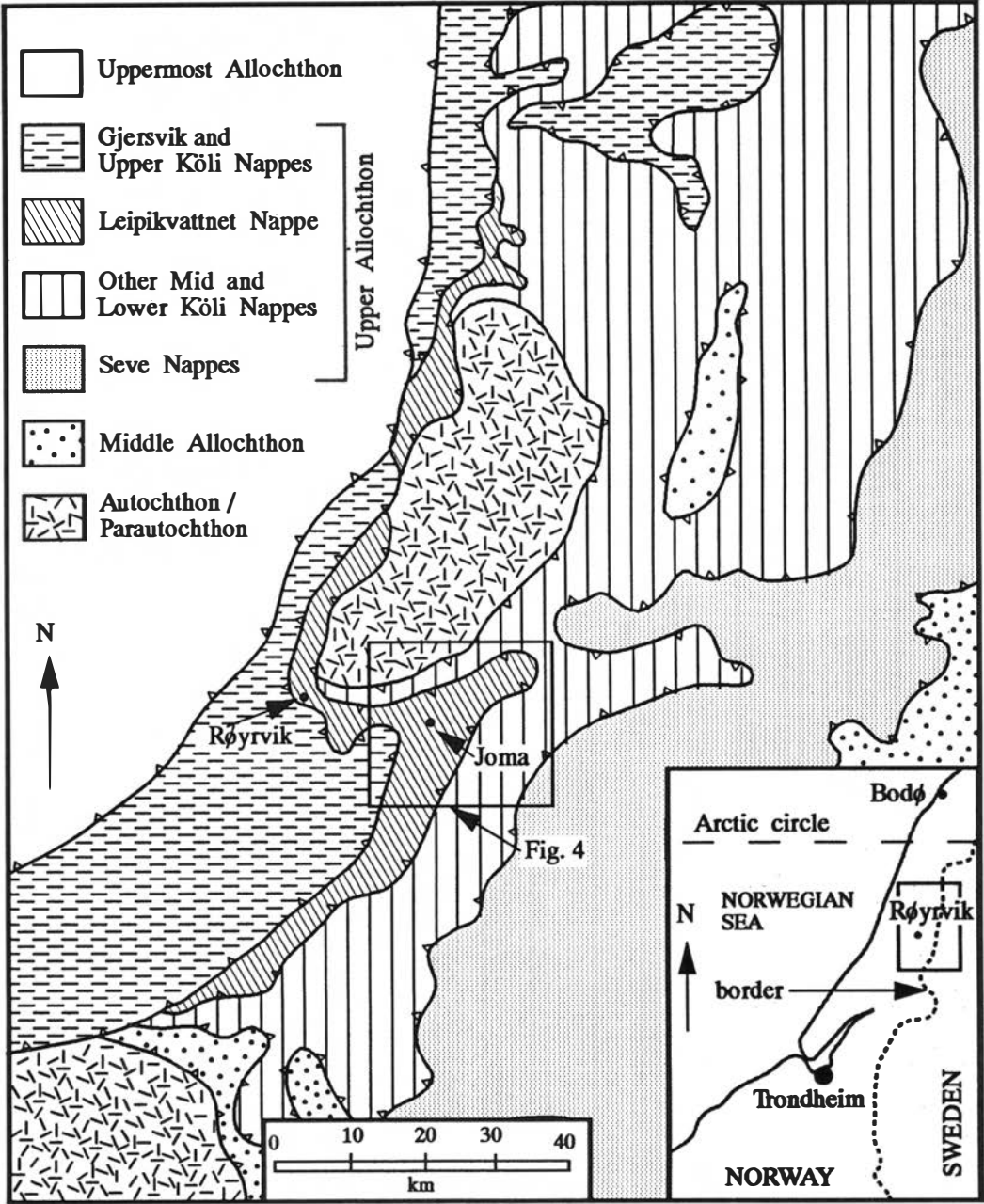
*Fig. 1.* Location of the Joma district relative to Trondheim and Røyrvik. Geological boundaries simplified from Stephens & Gee (1985), Stephens (1988) and Odling (1989).

out recourse to progressive flow or slip parallel to their axial surfaces (Turner & Weiss 1963, p. 487; Ramsay 1967, p. 434; Hobbs et al. 1976 pp. 195–199; but also note the model advocated by Hudleston 1977). In essence, apparent great-circle redistribution patterns of contoured linear elements neither require perfect similar geometry nor prove simple shear folding.

## Fold geometry in the Joma district

Based on dip isogon analysis (Fig. 3), mesoscale $F_3$ folds from various multilayers at and in the vicinity of Joma Mine have geometries ranging from class 1C (competent layers) to class 3 (incompetent layers). Such geometries are consistent with modified-parallel fold styles and initiate through buckling process (e.g. Ramsay 1967, pp. 431–432; Hobbs et al. 1976, p. 195). Further, because the folds have limited persistence within the axial surface normal to the hingeline, they do not even approximate similar geometry.

The same conclusion may be reached by examining the regional $F_3$ Joma Synform (e.g. Kollung 1979; Roberts 1979; Marshall et al. 1987; Odling 1988, 1989; Marshall 1990) (Fig. 4). The en echelon axial surface traces, the apparent class IC/3 geometry in plan and profile (less obvious), and the competence contrast under conditions
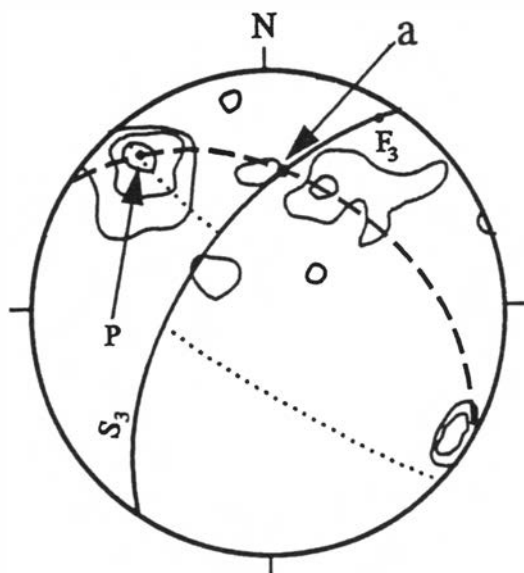
*Fig. 2.* A Lambert equal-area stereogram of $D_2$ linear fabric elements (62 points) from zone B of the Joma area (see Fig. 4) redistributed about the local $F_3$ hingeline; contours at 2-4-6 data points per 1% area; 'P' is the assumed pre-$D_3$ orientation of the $D_2$ linear elements. The small circle (dotted) and great-circle (dashed) are the theoretical redistribution loci for concentric folding and the simple shear fold mechanism. 'a' is the inferred shear direction during simple shear. Modified from Odling (1989).
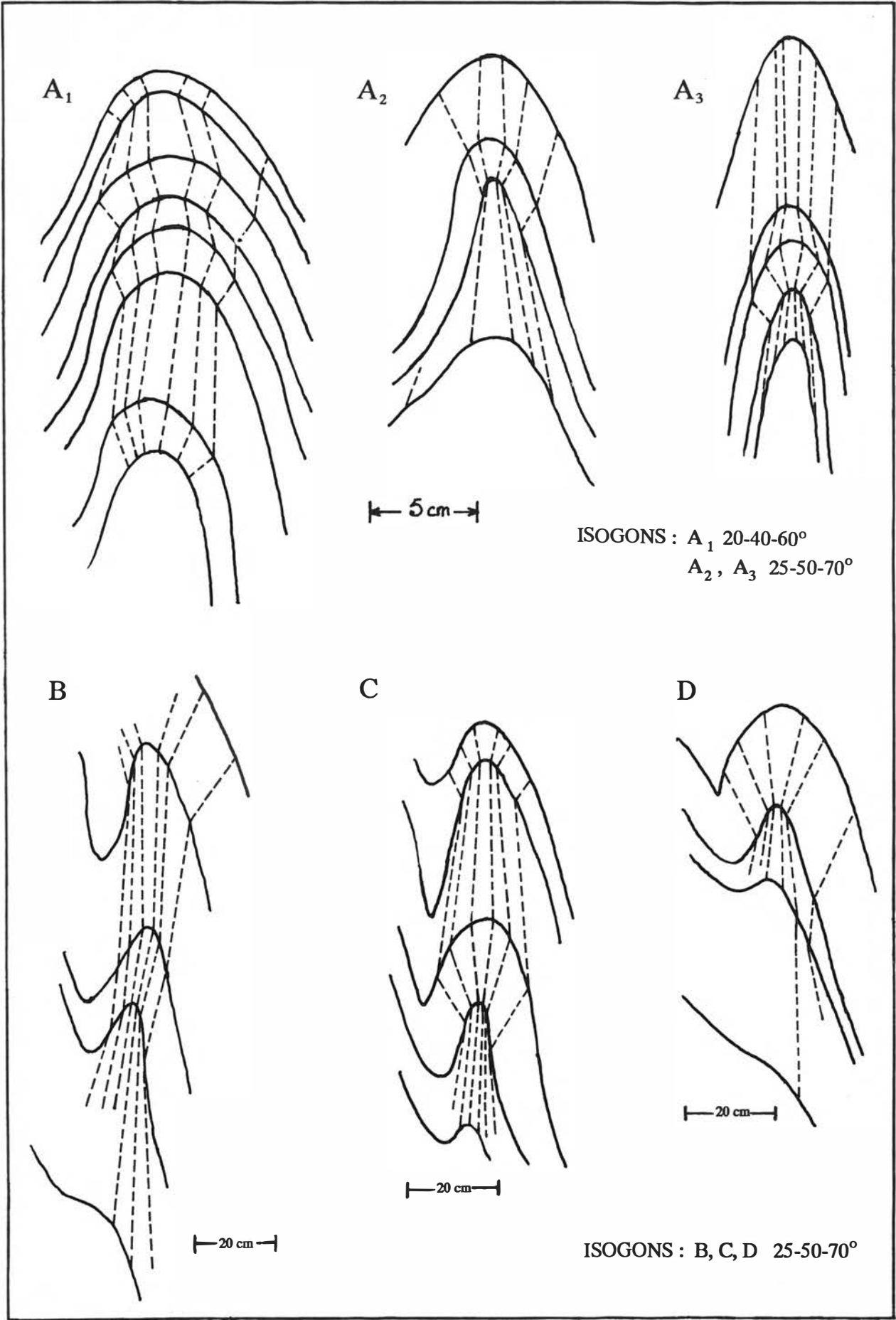
Marshall et al. 1987; Odling 1988, 1989; Marshall 1990), and, in contrast with what might be expected for a simple shear mechanism, the $D_3$ axial surface foliation is rarely penetrative (Odling 1989).

3. Redistribution data from two $F_3$ mesofolds in greenschist from Joma mine, which falls within Odling's critical zone B (1989, figs. 9 and 11), do not directly differentiate between buckling and inhomogeneous simple shear mechanisms (Fig. 5). This is because an approximate 90° relationship existed at mesoscale between $D_2$ and $D_3$ linear elements at this locality. However, should a simple shear mechanism be invoked, the redistribution patterns differ significantly from Odling's regional data in relation to the possible shear direction (cf. Figs. 2 and 5). In addition, because the two folds lack a penetrative axial surface foliation and possess a near-concentric geometry, it should be noted that they are incompatible with an inhomogeneous simple shear model.

The foregoing items strongly suggest that a $D_3$ fold mechanism dominated by across-layer inhomogeneous simple shear is inapplicable in the Joma district.

## Discussion and conclusions

Various combinations of non-commutative flexural slip and homogeneous flattening, flexural slip and across-layer simple shear, and buckling instability or across-layer simple shear with superimposed progressive inhomogeneous contraction, can all yield folds of approximately similar composite geometry, and can redistribute earlier rectilinear elements into near-great-circle patterns (Ramsay 1967). Careful selection of shear directions and strain axis orientations for the various components of strain enables any of these complex fold models to explain Odling's (1989) data, particularly when the geometries of the pre-$D_3$ form surface and linear elements are considered. However Figs. 2, 3 and 4 allow an interpretation which is in keeping with the competence contrasts and pre-$D_3$ geometry of the main lithological units. The regional sequence comprises intercalations of graphitic and quartz-rich phyllites, thin-bedded quartzites, and massive, pillowed and tuffaceous greenstones. Compared with the greenstones, the phyllites and thin-bedded quartzites were less competent and thereby weakly exhibit class 3 geometry. Within these less competent portions of the sequence, regional macrofolds could have involved a significant component of progressive inhomogeneous contraction (see Ramsay 1967, p. 484). This is despite mesofolds in thin competent layers within the same portion of the sequence having class IC geometry and being initiated by bucking. Since progressive inhomogeneous contraction redistributes lineations along complex loci akin to an incomplete great-circle pattern (Ramsay 1967, p. 485), $D_2$ linear elements from less competent portions of the Joma sequence could

of low grade metamorphism between massive and pillowed greenstone and graphitic and quartzose phyllites, all oppose true similar geometry produced by across-layer inhomogeneous simple shear.

### Redistribution geometry in the Joma district

Three aspects relating to redistribution geometry of the $D_2$ linear elements in the Joma district have bearing on the $D_3$ fold mechanism.

1. The pre-$D_3$ orientation of $D_2$ linear elements is uncertain (Odling 1989). A shallow NW plunge is dominant in regions where $D_3$ influence is deemed minimal, but evidence exists (Marshall 1990) for a pre-$D_3$ great-circle dispersion of $D_2$ linear elements. Given these factors, plus the inconsistent orientation of $D_3$ hinge lines (Marshall 1990), the redistribution geometry of $D_2$ about $D_3$ should not be interpreted as a simple great-circle pattern.
2. Many natural folds displaying combinations of classes (e.g. IC/3), result from buckling instability followed by flattening and simple shear modifications parallel to the axial surface (e.g. Turner & Weiss 1963, pp. 487–490; Donath & Parker 1964; Ramsay 1967, pp. 482–486). In particular, Ramsay portrayed various combinations of flexural slip and simple shear that might explain Odling's results (1989, fig. 11), provided that 'a' (Fig. 2) constituted the shear direction. However, evidence supporting this shear direction (such as elongation lineation paralleling 'a' in the $D_3$ axial surfaces) has not been reported (e.g. Olsen 1980;

ISOGONS : $A_1$ 20-40-60°
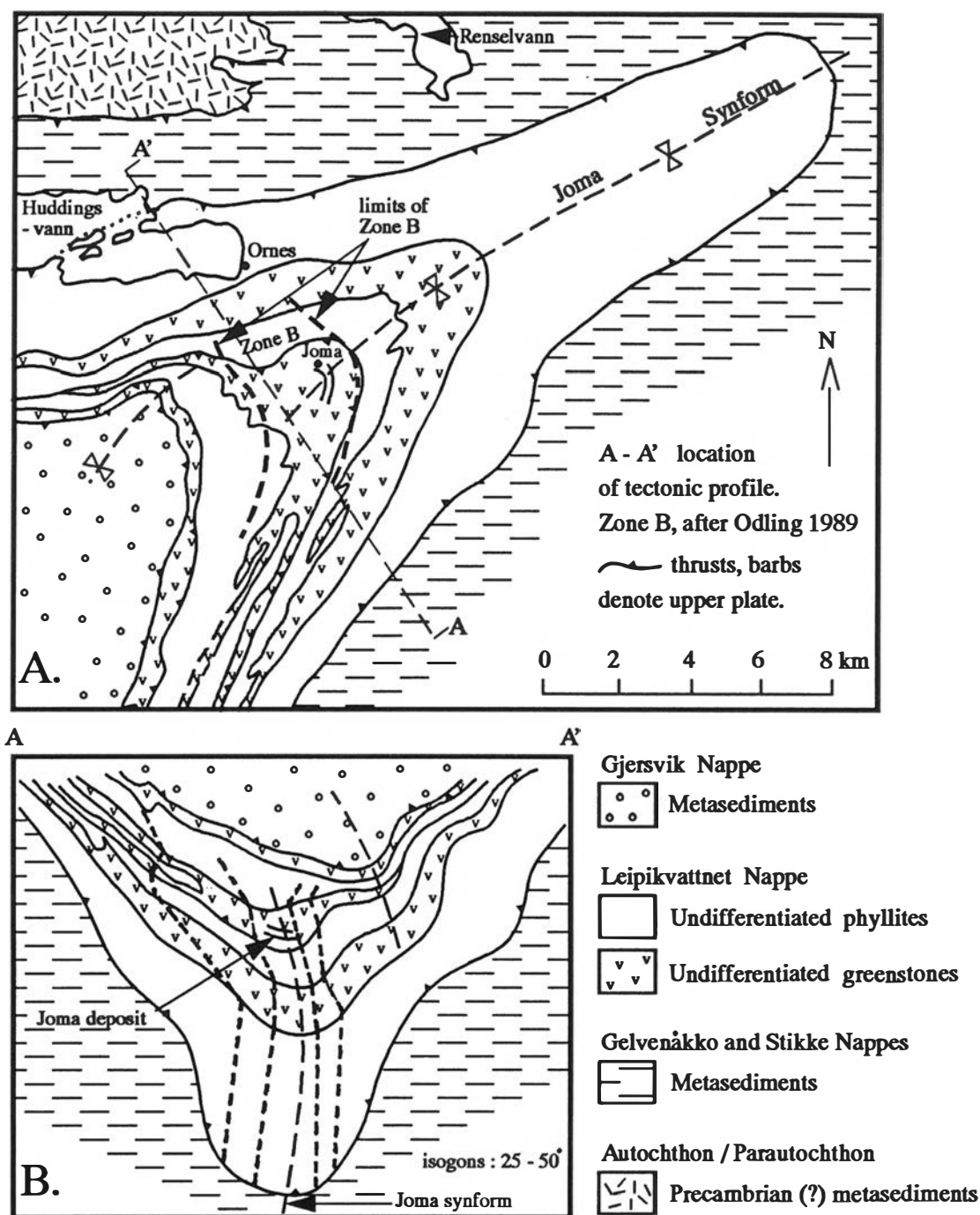$A_2$, $A_3$ 25-50-70°

ISOGONS : B, C, D 25-50-70°

*Fig. 4.* A. Geological map of the F₃ Joma Synform, as modified from Kollung (1979), Reinsbakken & Stephens (1986), and Fossen & Kollung (1988); see Fig. 1 for locality map. B. Structural profile and dip isogon analysis of the Joma Synform; constructed along A-A' (Fig. 4A).

yield such a distribution. Thus, provided that a substantial proportion of the $D_2$ data were derived from less competent sources (as is implied by Odling 1984, 1989, pers. comm. 1991), it is possible to reconcile an approximate

*Fig. 3.* Dip isogon analysis of mesoscale F₃ folds in multilayers from the Joma district. A, in quartzose phyllites; comprising alternating quartz-rich (Class 1 isogons) and quartz-poor (Class 3) layers; surface exposure approximately 2 km WNW of Joma opencut. B, in alternating pyritic ore (Class 1) and chlorite-rich greenstone (Class 2/3); C, in pyritic ore (Class 1, top layer), carbonate rock (Class 1, middle layer) and chlorite-actinolite schist (Class 3); D, in albite laminite (Class 1), chlorite schist (Class 3) and pyritic ore (bottom layer); B, C and D from 387 level, Joma Mine.
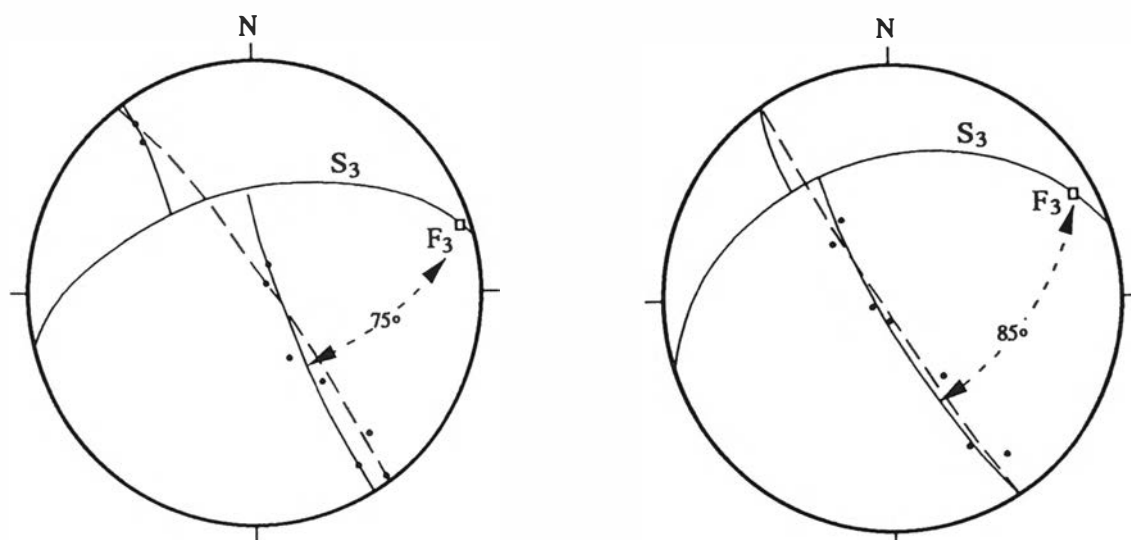
great-circle redistribution pattern with a fold style requiring buckling processes.

Extending the interpretation further, strain X and 'a' for the components of the inhomogeneous contraction throughout much of the region would have been approximately normal to the SW plunging regional F₃ hingeline. However, in zone B (Odling 1989, figs. 9, 11; Fig. 4), although strain X and 'a' remained constantly oriented, the F₃ hingeline reversed its plunge, this probably being due to a local variation in form surface orientation (an interpretation also made by Odling 1989), since zone B

*Fig. 5.* Lambert equal-area stereograms of two $F_3$ mesofolds and their redistributed $D_2$ linear elements (dots); the best fit small-circle (continuous) and great-circle (dashed) redistribution loci are indicated.
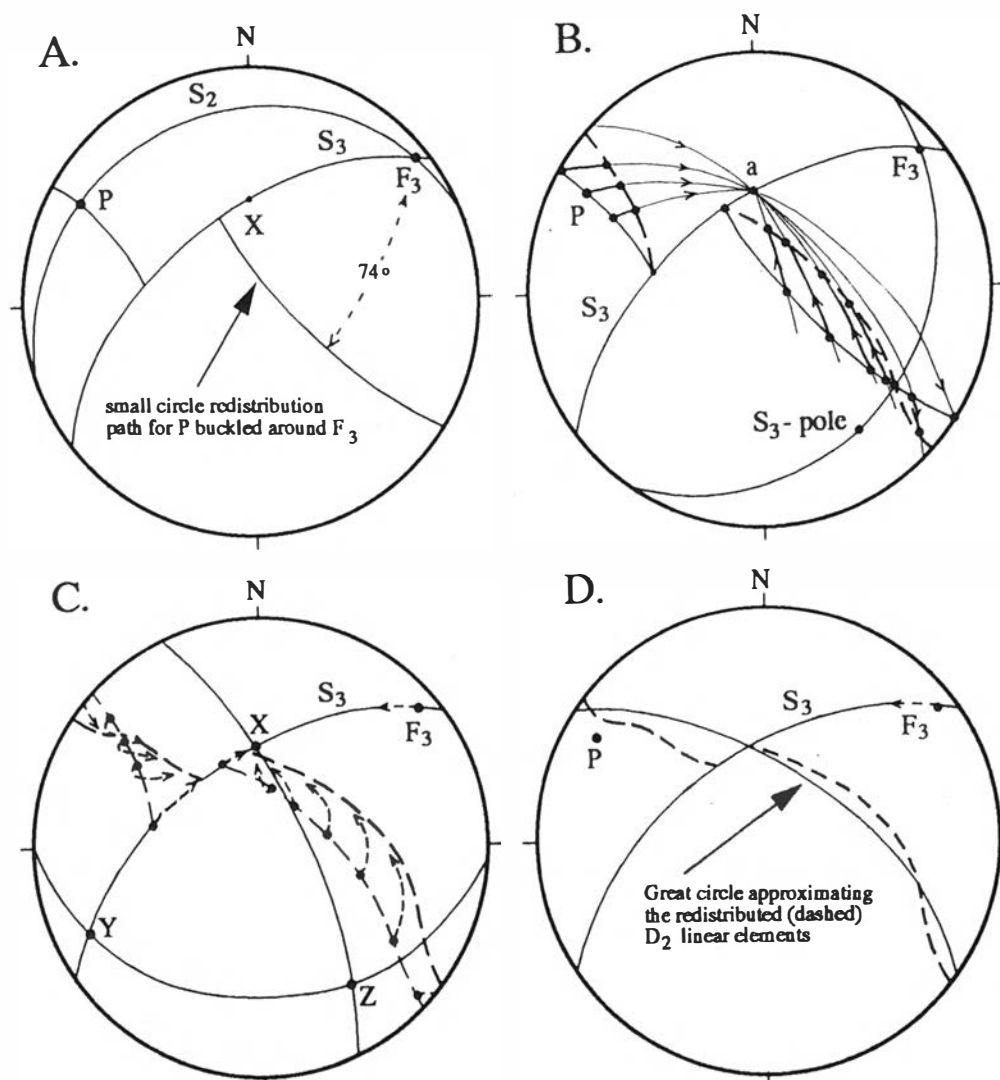


*Fig. 6.* Lambert equal-area projections of the progressive redistribution of $D_2$ linear elements by the interpreted $D_3$ fold mechanism: $S_2$ – inferred orientation of the $F_3$ form surface; 'P' – assumed pre-$D_3$ orientation of the $D_2$ linear elements; $F_3$, $S_3$ – $D_3$ hingeline and axial surface; X, Y, Z – inferred principal axes of strain; 'a' – inferred shear direction in $S_3$. A. Redistribution by asymmetric buckling. B. Redistribution trajectories (arrows) and possible loci (dashed) resulting from inhomogeneous simple shear. C. Possible redistribution trajectories (arrows) for inhomogeneous pure strain of loci from B – possible new loci shown by heavy dashes. D. Great-circle approximating the new loci from C.

centres upon an $F_2$ macrofold preserved within a lenticular body of greenstone.

The above interpretation is presented on a series of equal-area stereographic projections (Fig. 6). $S_2$ and the $D_2$ linear elements are folded by an initial component of SE-verging asymmetric buckling (Fig. 6A), as would have evolved in the competent layers and been transferred into the incompetent layers. The resulting small-circle distribution of $D_2$ linear elements is modified in the incompetent layers by a progressive inhomogeneous contraction which, in accordance with Ramsay (1967, pp. 484–485), is imposed as an inhomogeneous simple shear parallel to the fold axial surface (Fig. 6B) followed by an inhomogeneous pure strain with Z normal to the axial surface (Fig. 6C). Again following Ramsay (1967, p. 485), strain X is made to parallel the slip direction 'a' of the shear component. The pattern of $D_2$ linear elements arising from this deformation can be approximated by a great-circle of similar orientation to that in Fig. 2 (Fig. 6D). Partly based on Odling (1989) and Marshall (1990), assumptions have been made regarding the pre-$D_3$ orientations of $S_2$ and $D_2$ linear elements, and the orientations of $F_3$, $S_3$, 'a' and strain X. The selected values result in the $D_3$ redistribution of $D_2$ linear elements being consistent with the field relationships. Nevertheless, the result is moderately insensitive to reasonable variations of the selected values, particularly since, by its very nature, a progressive inhomogeneous contraction can not be specified in detail.

The $D_3$ fold style and the great-circle redistribution geometry at Joma may be reconciled by differing combinations of buckling and inhomogeneous contraction in the competent and less competent portions of the regional sequence. The less competent portions were dominated by inhomogeneous contraction such that $D_2$ linear elements rotated towards an approximate great-circle pattern. The more competent portions were dominated by flexural processes and underwent little modification by inhomogeneous contraction. Only where the angle between the $D_3$ hingeline and $D_2$ linear elements was substantially less than 90°, was it possible to appreciate the role of inhomogeneous contraction. There is no justification, either generally or at Joma, for unquestioningly equating an approximate great-circle redistribution of linear elements with a fold mechanism involving across-layer simple shear.

Understanding the $D_3$ fold mechanism has bearing on kinematic interpretation within the Upper Allochthon (Fig. 1) of the central Scandinavian Caledonides (e.g. see the discussion in Odling 1989). It also enables a better understanding of remobilization geometry (and thereby development needs) within the Joma orebody.

# References

Donath, F. A. & Parker, R. B. 1964: Folds and folding. *Geological Society of America Bulletin 75,* 45–62.

Fossen, H. & Kollung, S. 1988: Jomafjellet berggrunnskart 1924, 1, 1:50,000, foreløpig utgave Norges geologiske undersokelse.

Hobbs, B. E., Means, W. D. & Williams, P. F. 1976: *An Outline of Structural Geology,* 571 pp. John Wiley, New York.

Hudleston, P.J. 1977: Similar folds, and gravity tectonics in ice and rocks. *Journal of Geology 85,* 113–122.

Kollung, S. 1979: Stratigraphy and major structures of the Grong district, Nord-Trøndelag. *Norges geologiske undersokelse 354,* 1–51.

Marshall, B. 1990: 'Pseudostratigraphy' and thrusting in relation to the structural evolution of the Joma ore body, North Trøndelag, Norway. *Ore Geology Review 5,* 175–219.

Marshall, B. & Gilligan, L. B. 1989: Durchbewegung structure, piercement cusps, and piercement veins in massive sulfide deposits: formation and interpretation. *Economic Geology 84,* 2311–2319.

Marshall B., Odling, N. E., Reinsbakken, A. & Vokes, F. M. 1987: Pseudo-stratigraphy and thrusting at Joma Mine, Norway. *Geological Society of Australia Abstracts 19,* 112–115.

Odling, N. E. 1984: *The structure of the Joma massive sulphide deposit and surroundings.* Unpublished report, Grong Gruber A/S (November), 16 pp.

Odling, N. E. 1988: Deformation of the Joma sulphide deposit, Caledonides of N. Trondelag, Norway. *Proceedings of the Seventh Quadrennial IAGOD Symposium,* 513–524. E. Schweizerbart'sche, Stuttgart.

Odling, N. E. 1989: The structural history of the Leipikvattnet Nappe in the Joma area of Nord Trøndelag, central Scandinavian Caledonides, Norway. *Norsk Geologisk Tidsskrift 68,* 141–161.

Olsen, J. 1980: Genesis of the Joma stratiform sulphide deposit, central Scandinavian Caledonides, *Proceedings of the Fifth Quadrennial IAGOD Symposium,* 745–757. E. Schweizerbart'sche, Stuttgart.

Ramsay, J. G. 1960: The deformation of early linear structures in areas of repeated folding. *Journal of Geology 68,* 75–93.

Ramsay, J. G. 1967: *Folding and Fracturing of Rocks,* 568 pp. McGraw-Hill, London.

Ramsay, J. G. & Huber, M. I. 1987: *The Techniques of Modern Structural Geology, vol. 2: Folds and Fractures,* 700 pp. Academic Press, London.

Reinsbakken, A. & Stephens, M. B. 1986: Lithology and deformation in the massive sulphide-bearing Gelvenakko and Leipikvattnet Nappes. *In* Stephens, M. B. (ed.): Stratabound sulphide deposits in the central Scandinavian Caledonides, *Sveriges geologiska undersokning Ca60,* 42–45.

Roberts, D. 1979: Structural sequence in the Limingen-Tunnsjøen area of the Grong district, Nord-Trøndelag. *Norges geologiske undesøkelse 354,* 101–114.

Stephens, M. B. 1988: The Scandinavian Caledonides: a complexity of collisions. *Geology Today (Jan-Feb),* 20–26.

Stephens, M. B. & Gee, D. G. 1985. A tectonic model for the evolution of the eugeoclinal terranes in the Central Scandinavian Caledonides. *In* Gee, D. G. & Sturt, B. A. (eds.): *The Caledonian Orogen: Scandinavia and Related Areas,* 953–978. Wiley, New York.

Turner, F. J. & Weiss, L. E. 1963: *Structural Analysis of Metamorphic Tectonites,* 545 pp. McGraw-Hill, New York.